Fan Noise Predictions of the NASA Source Diagnostic Test using Unsteady Simulations with LAVA Part I: Near-Field Aerodynamics and Turbulence

Luis S. Fernandes†, Jeffrey A. Housman

Gaetan K. Kenway†, Gerrit-Daniel Stich†, Cetin C. Kiris

Aerosciences Branch, NASA Ames Research Center

AIAA SciTech Forum, January 23-27 2023

National Harbor, MD

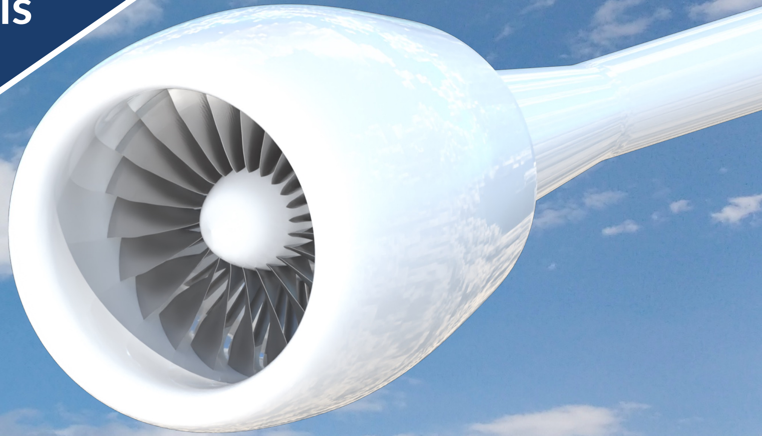

†Science and Technology Corp.

Motivation

- Trends in commercial aviation turbofan efficiency continue to favor the development of ultra-high bypass ratio turbofan engines as a near-term solution to tackle low-noise demands in urban traffic areas
- This leads to higher fan-to-jet noise ratios during take-off and approach, motivating work towards fully characterizing the noise signature of rotating fan rigs
- A sliding mesh technique has been implemented in the LAVA solver framework, and this study aims at validating the methodology in a complex geometry setting

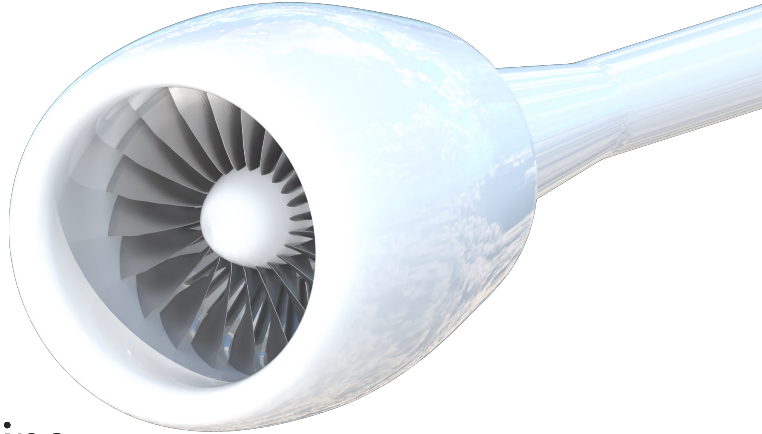

Render of NASA SDT baseline geometry

NASA Source Diagnostic Test (SDT)

- 22” fan rig mounted on the 9x15 ft. Low Speed Anechoic Wind Tunnel (LSWT)
- Baseline configuration: 22 fan/54 OGV blades
- Low-speed (approach) condition
- High-speed (take-off) condition
- Vast experimental dataset:
  - Fan stage performance metrics
  - Mean and turbulent flow interstage characterization
  - Acoustic Sound Pressure Level (SPL) measurements along a sideline microphone array (focus of Part II)

Credit: C. Hughes (NASA GRC)

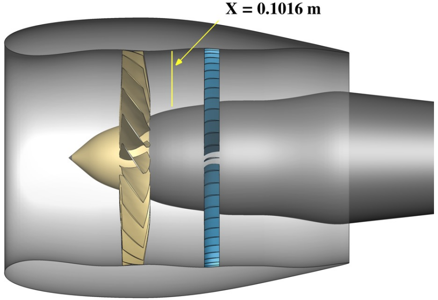

Hot-wire station 1 location

Launch, Ascent, and Vehicle Aerodynamics (LAVA) solver framework

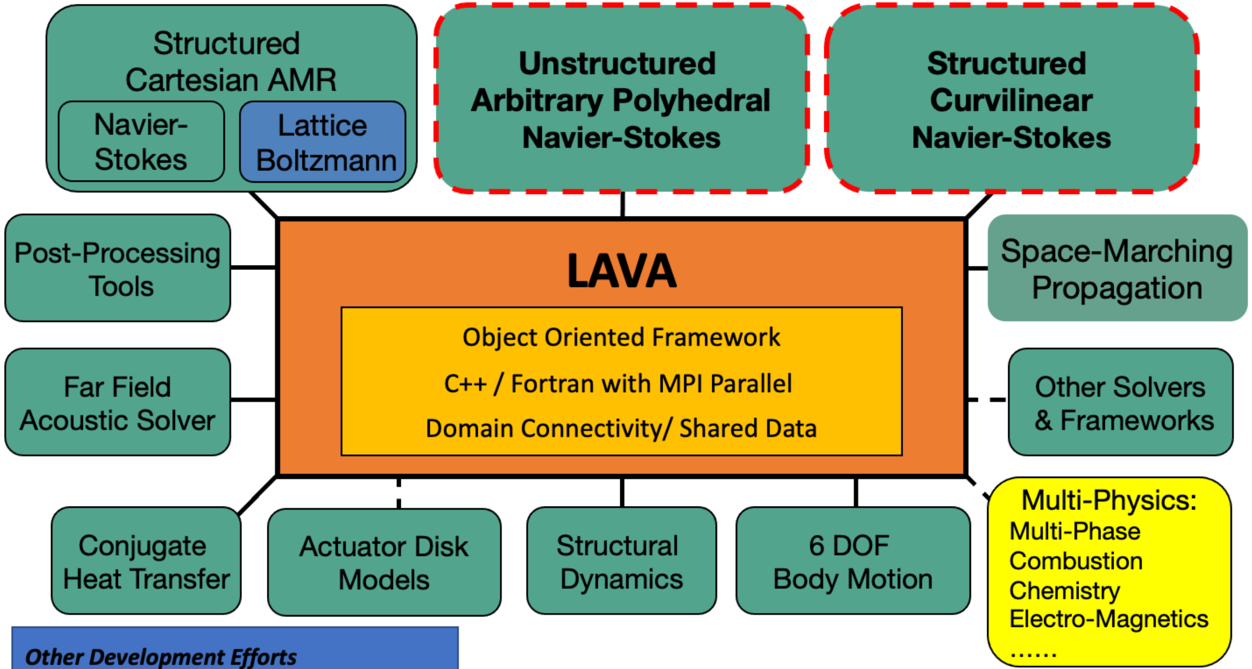

Other Development Efforts
- Higher order and low dissipation
- Curvilinear grid generation
- Wall modeling
- LES/DES/ILES Turbulence
- HEC (optimizations, accelerators, etc.)

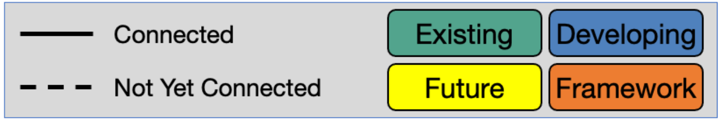

Kiris at al. AIAA-2014-0070 & AST-2016

Numerical Discretization

- Launch, Ascent, and Vehicle Aerodynamics (**LAVA**) solver framework
- Conservative finite-difference formulation applied to strong conservation law form of flow equations in curvilinear coordinates
- Overset grid paradigm used to discretize computational domain
- 2^{nd} order implicit **BDF2** time-stepping
- 2^{nd} order convective flux discretization
  - Modified Roe scheme
  - Blended 3^{rd} order upwind-biased and 4^{th} order central differencing operators
    - **URANS** Blending factor 1 % upwind everywhere
    - **HRLES** Blending factor 1 % upwind in LES regions ($f_d > 0.8$), pure upwind in RANS regions

Turbulence Model Closures

- **URANS** Unsteady Reynolds-Averaged Navier Stokes
  - Favre-Averaged RANS equations
  - Spalart-Allmaras (SA) turbulence model closure
    - **5 variants tested**: Baseline (SA), Baseline w/ Rotation/Curvature correction (SA-RC), Baseline w/ Quadratic Constitutive Relation, version 2000 (SA-QCR), Baseline w/ RC + QCR corrections (SA-RC-QCR) and Baseline w/ Mixing Layer Compressibility correction (SA-CC)

- **HRLES** Hybrid RANS/Large-Eddy Simulation
  - Zonal Detached Eddy Simulation (ZDES)
  - Shielding function protects attached boundary layers from LES mode
  - ZDES2020-Mode2-EP – Enhanced Protection model by Deck & Renard[1]
  - Baseline SA closure used in RANS mode (best-practice after sensitivity study)

[1] 10.1016/j.jcp.2019.108970

Overset Grid Topology

Slice along grid meridional plane emphasizing grid topologies employed

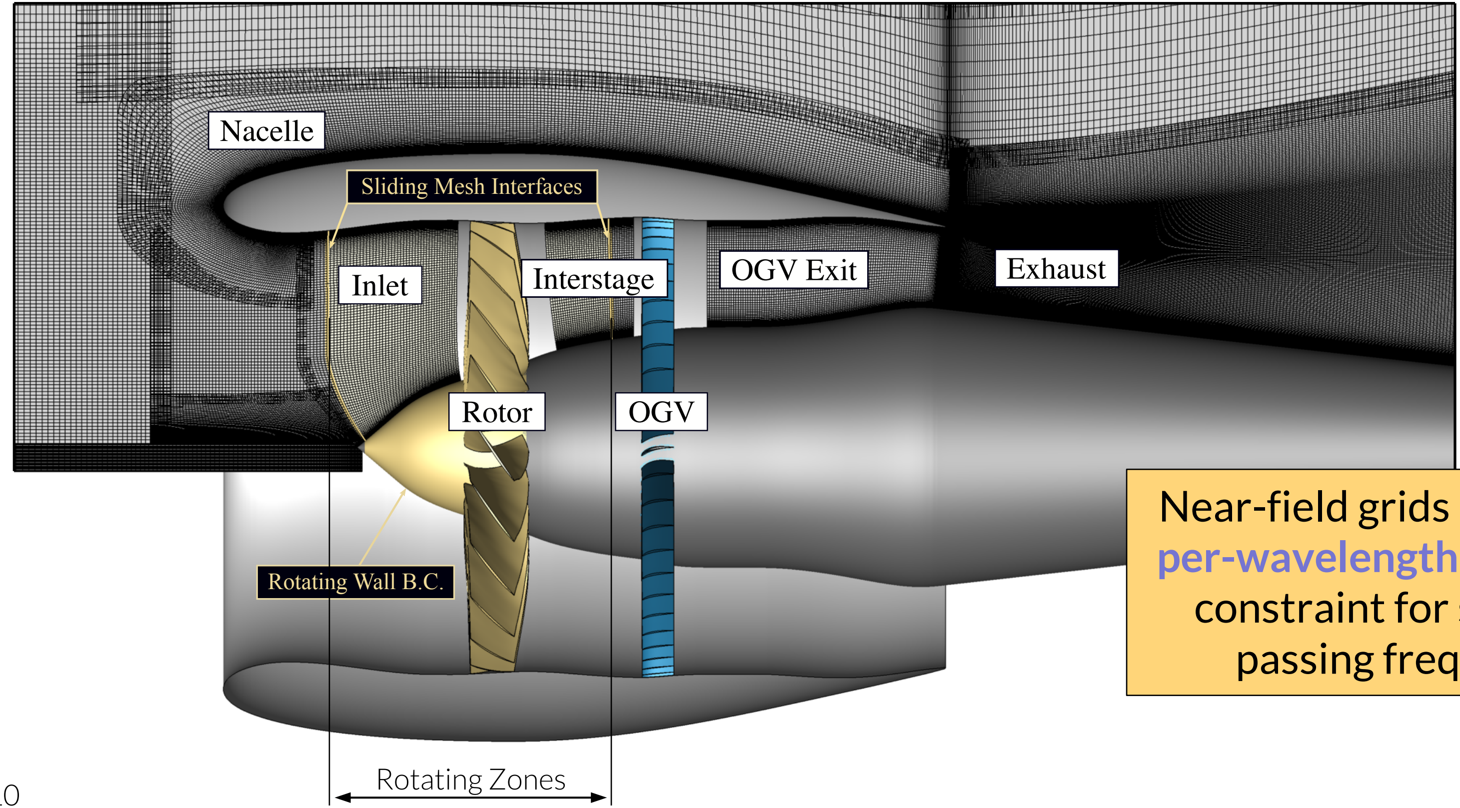

Near-field grids obey 15 points-per-wavelength (PPW) acoustic constraint for second blade-passing frequency BPF_2

Grid Refinement Study

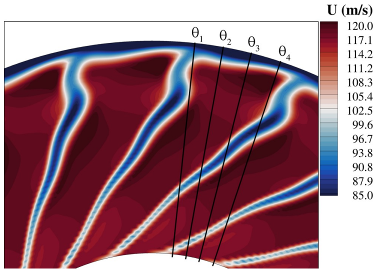

- Little grid sensitivity observed with URANS in performance metrics and velocity profiles
- Results support using the **Medium grid level** (385M solve points) for production runs, as it obeys 15 PPW for BPF_2

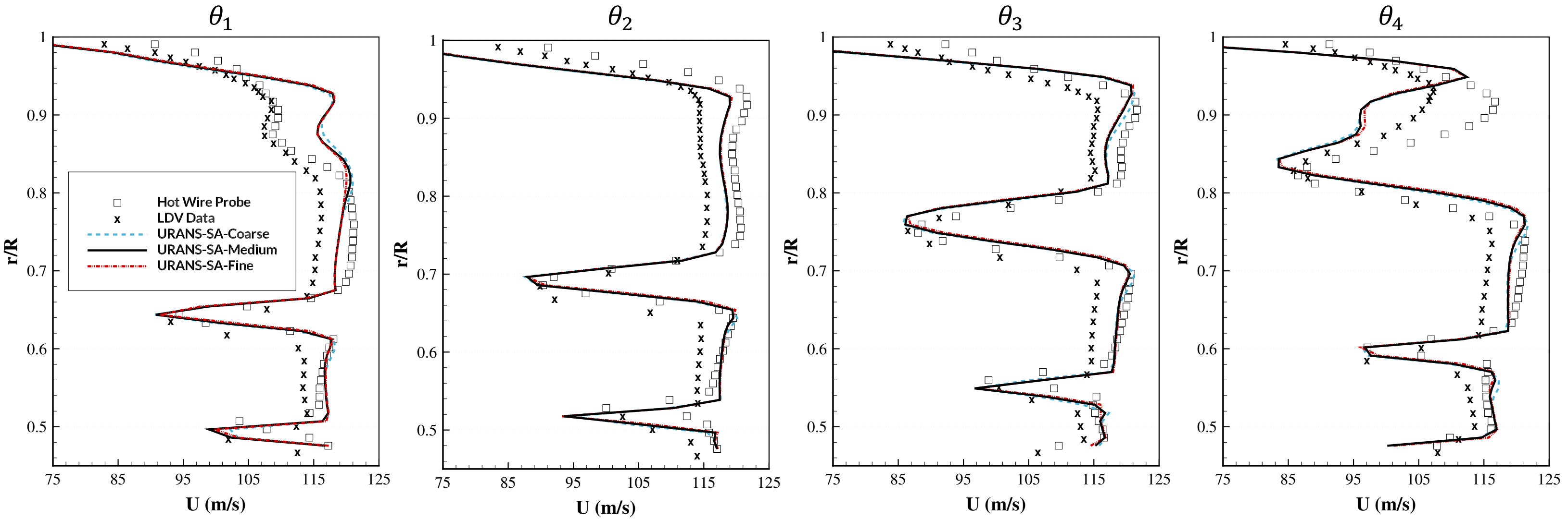

Mean **streamwise velocity** along radial lines. Computations compared to experimental data

Grid Refinement Study

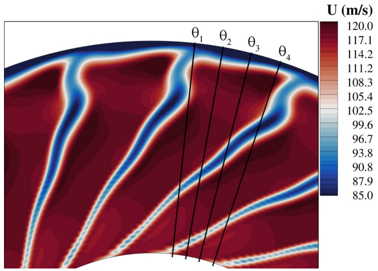

- Little grid sensitivity observed with URANS in performance metrics and velocity profiles
- Results support using the Medium grid level (385M solve points) for production runs, as it obeys 15 PPW for BPF_2

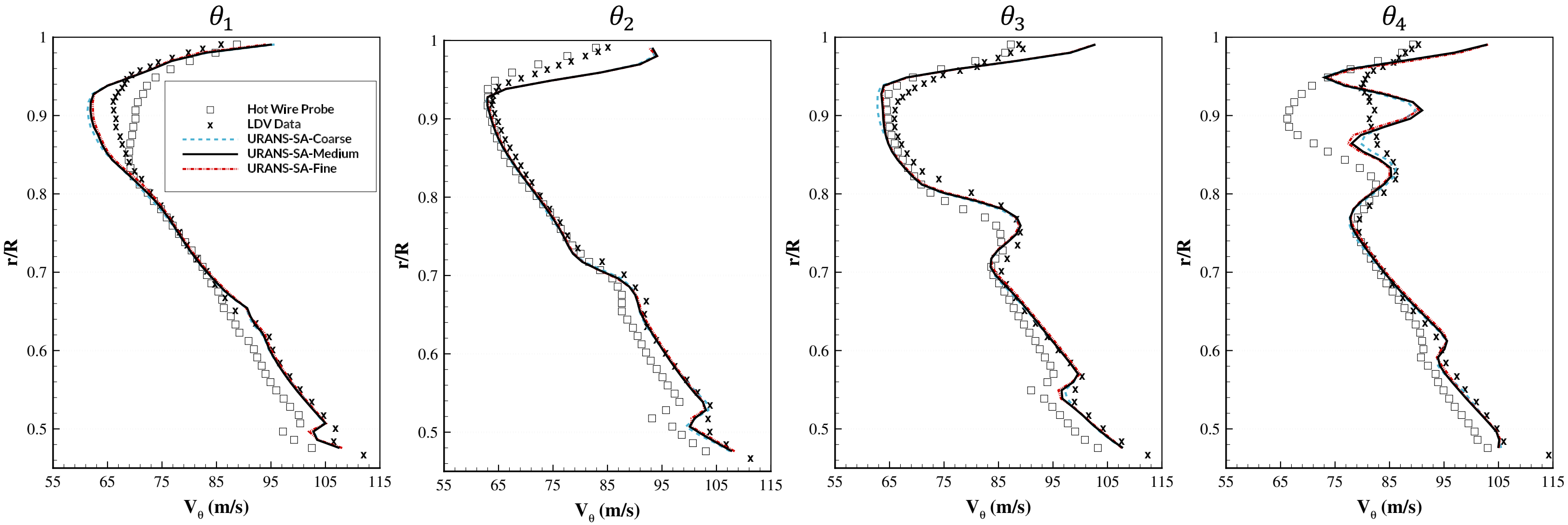

Mean azimuthal velocity along radial lines. Computations compared to experimental data

Grid Refinement Study

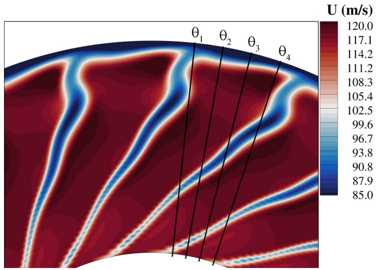

- Little grid sensitivity observed with URANS in performance metrics and velocity profiles
- Results support using the Medium grid level (385M solve points) for production runs, as it obeys 15 PPW for BPF_2

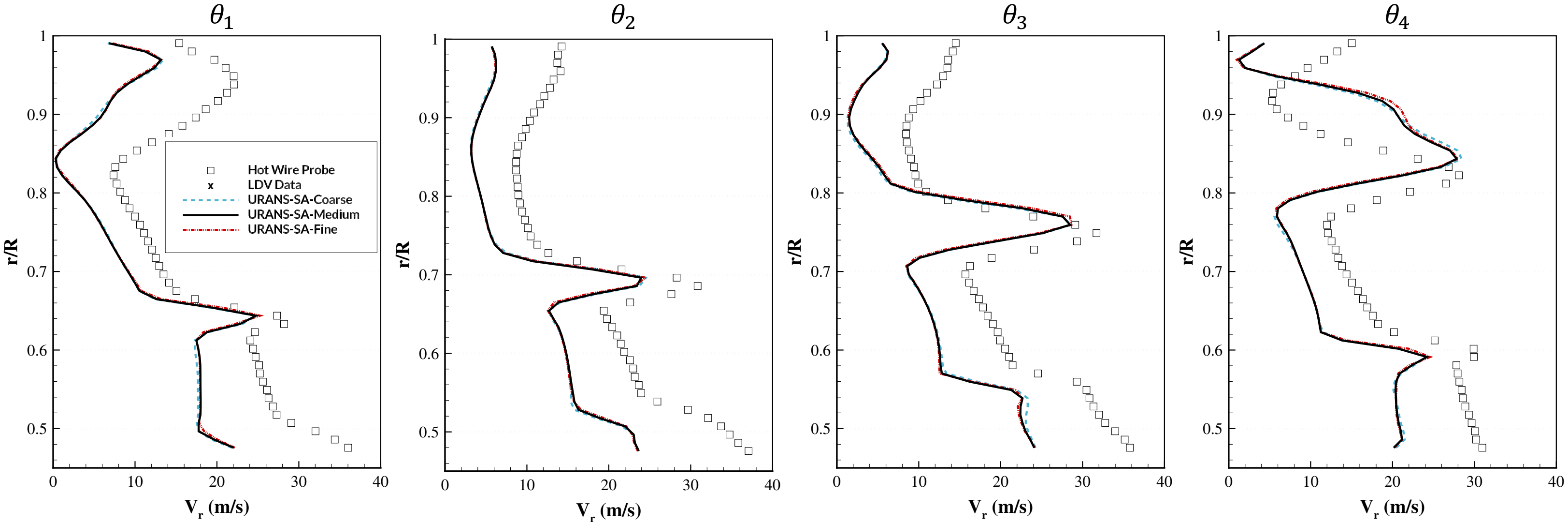

Mean radial velocity along radial lines. Computations compared to experimental data

Grid Refinement Study

Pressure Coefficient

Axial Skin Friction Coefficient

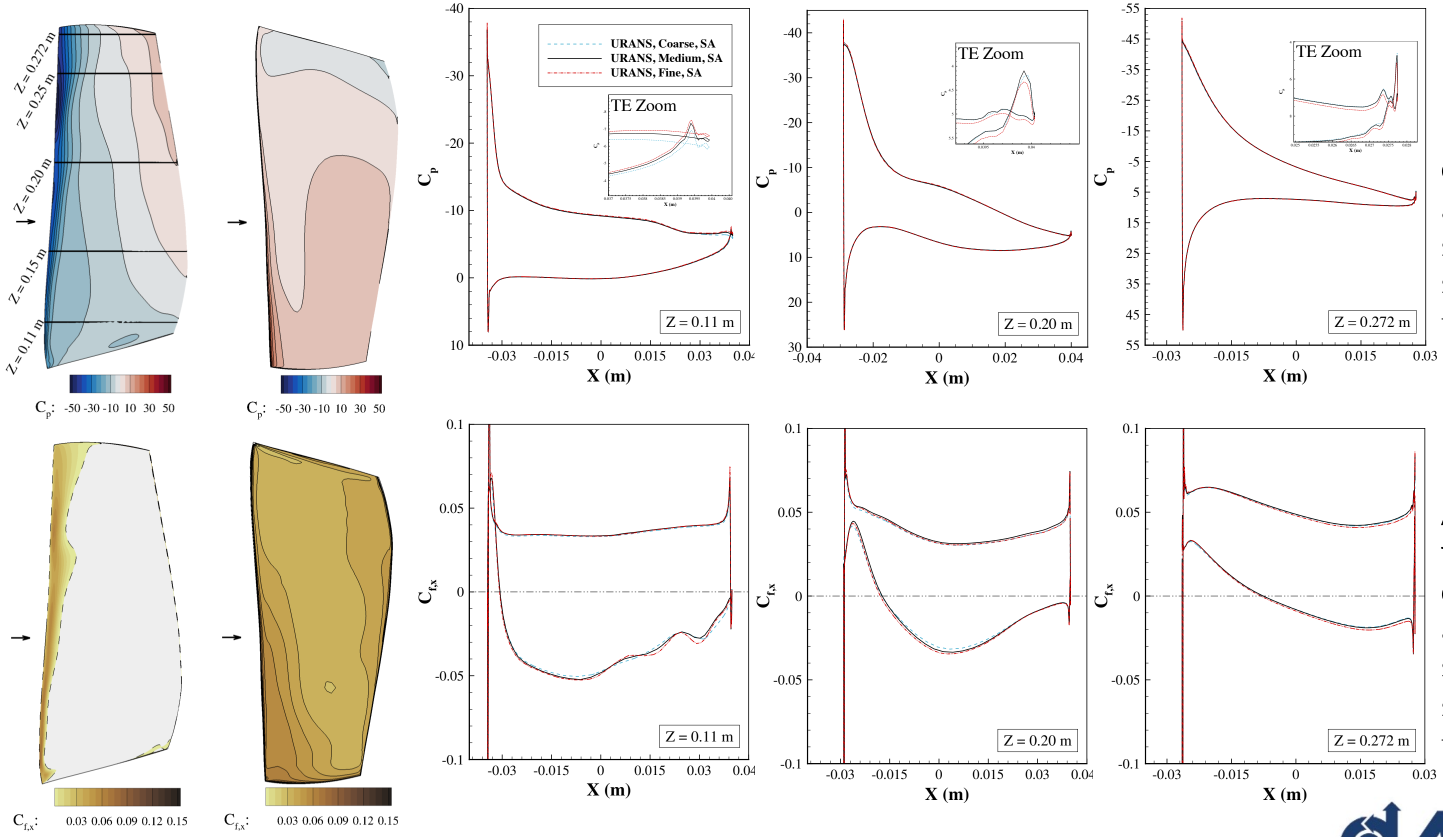

Pressure coefficient along several spanwise stations along the blade

Axial skin friction coefficient along several spanwise stations along the blade

Turbulence Model Sensitivity Study

- SA-RC-QCR turbulence model closure showed presence of strong spurious tones in acoustic signal produced by fan rig
- This led us to investigate the interstage flow-field, where we found large-scale unsteady vortical features not present in the SDT data
- Interaction of these vortices with downstream OGVs likely causing strong tones at frequencies other than blade-passing-frequency (BPF) harmonics

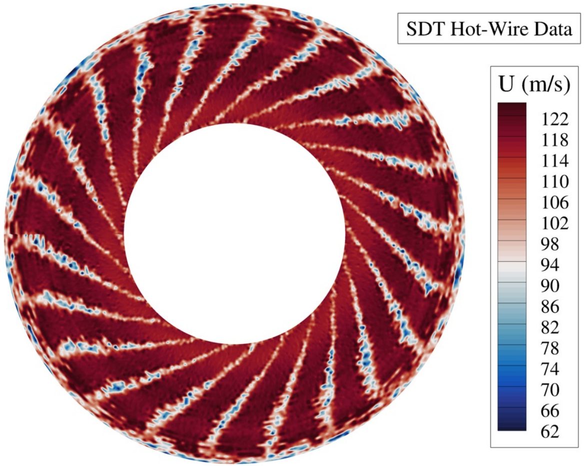

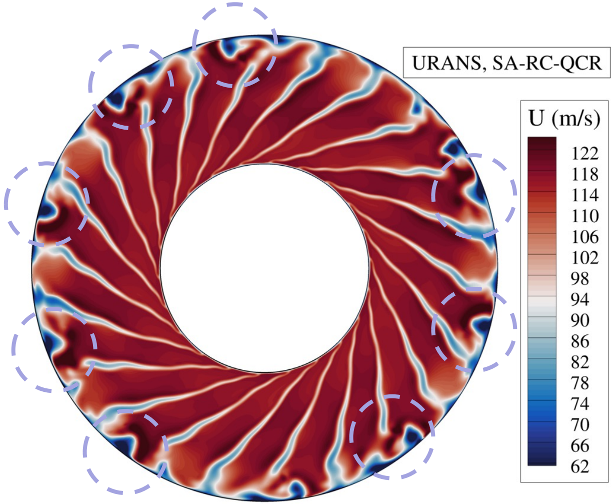

Mean axial velocity at hot-wire station 1

Turbulence Model Sensitivity Study

- Region downstream of blade tip extremely sensitive to turbulence model closure chosen
- Baseline SA model predicted a steady flow-field in the rotating frame - **chosen as best-practice**

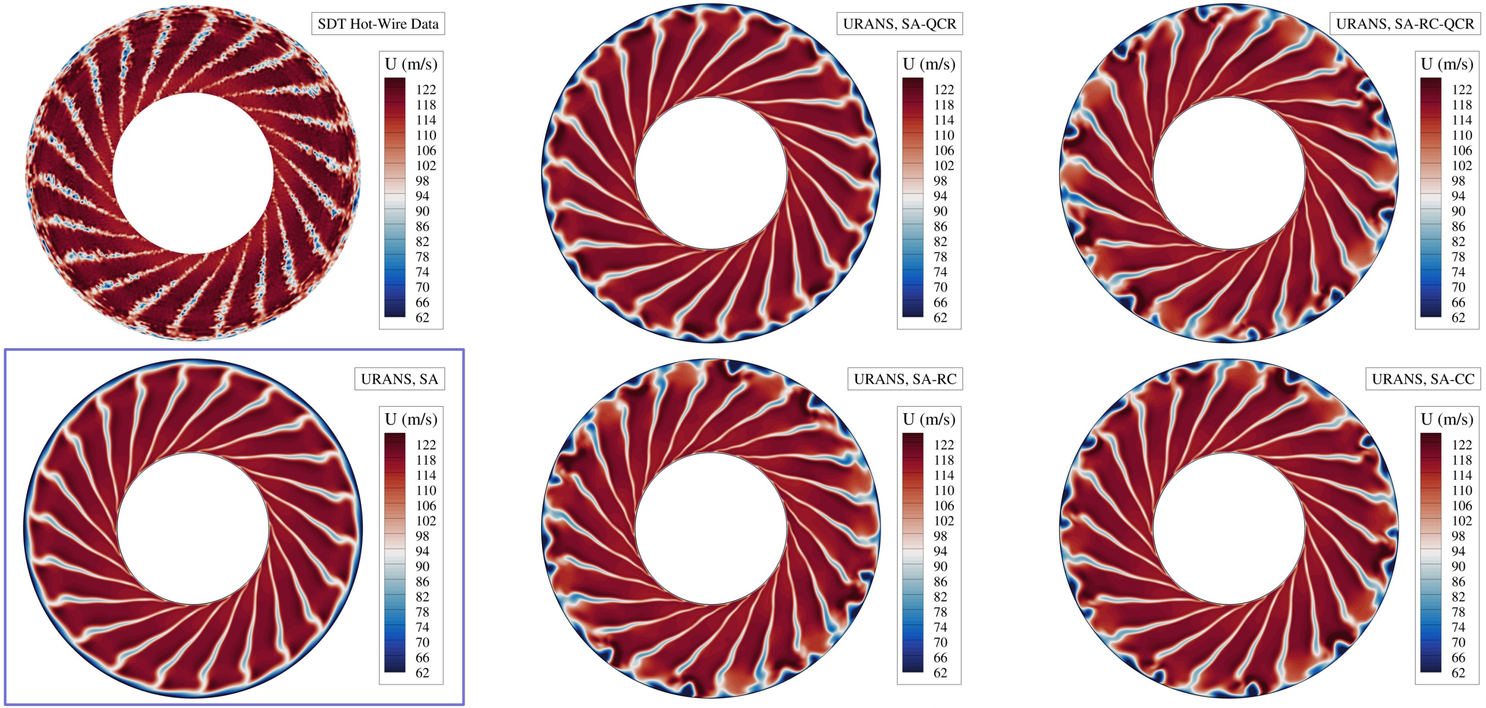

Mean axial velocity at hot-wire station 1

Low-Speed (Approach) Condition

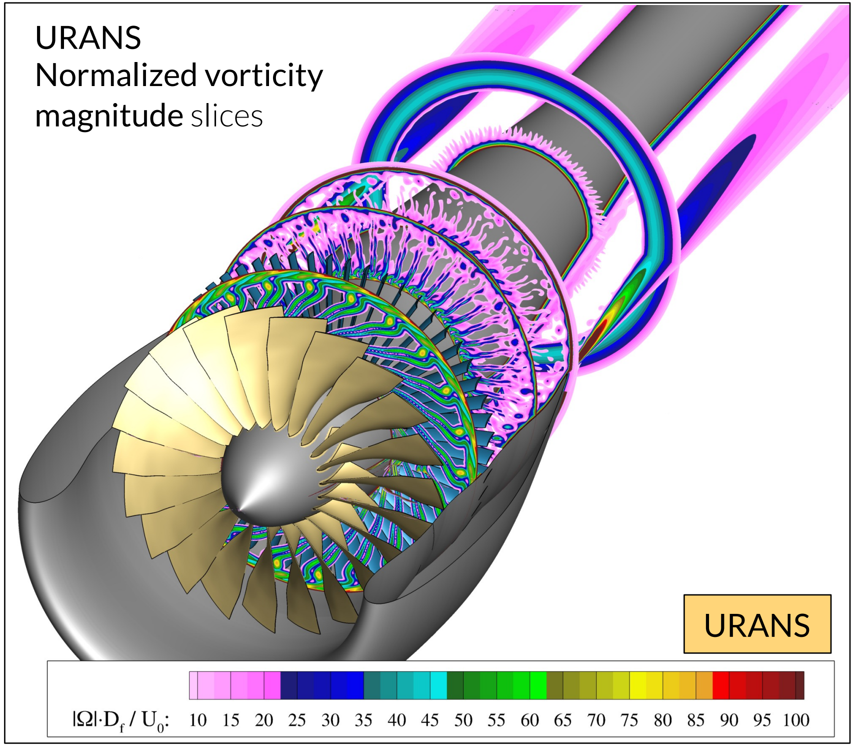

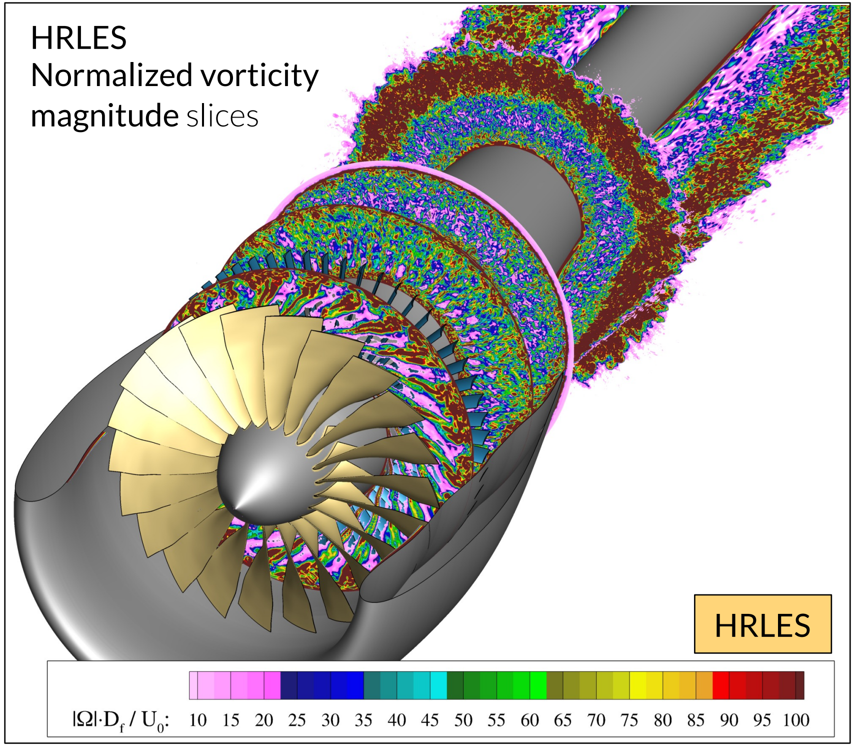

Significant differences in small-scale turbulent content predicted by the two models

Low-Speed (Approach) Condition

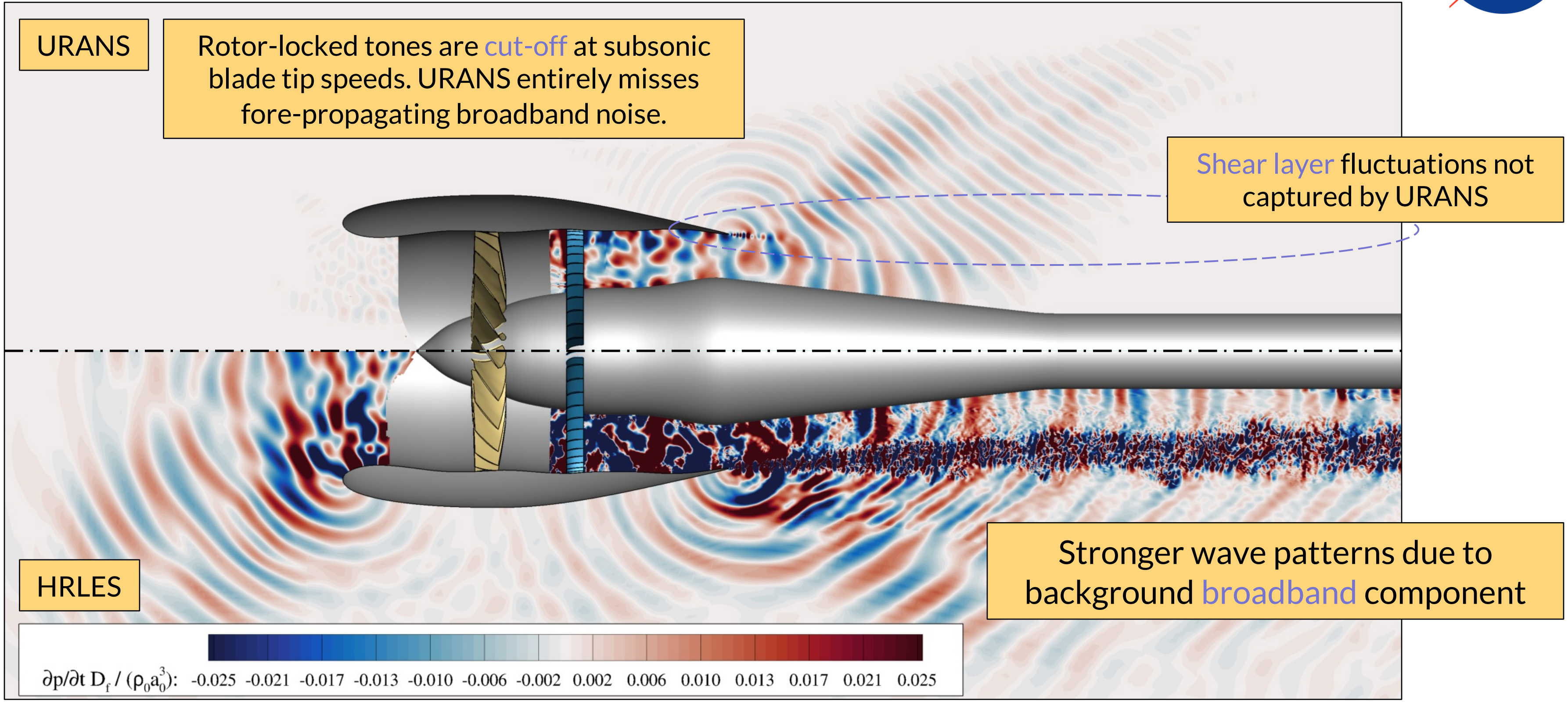

Sounds wave patterns predicted by URANS (top) and HRLES (bottom)

Low-Speed (Approach) Condition

Tim Sandstrom render video at low-speed

Video legend

Low-Speed (Approach) Condition

- Performance metrics show excellent agreement with SDT data (< 1%):

Case	Mass Flow Rate		Total Pressure Ratio		Total Temperature Ratio	
	Value [kg/s]	Δ [†]	Value	Δ	Value	Δ
SDT Data	**26.535**	-	**1.154**	-	**1.049**	-
URANS (SA)	26.779	+0.92 %	1.160	+0.6 %	1.050	+0.1 %
HRLES	26.780	+0.92 %	1.161	+0.6 %	1.050	+0.1 %

[†] Percent difference relative to the SDT data

Low-Speed (Approach) Condition

- Good agreement obtained in the interstage mean velocity flow-field for both models

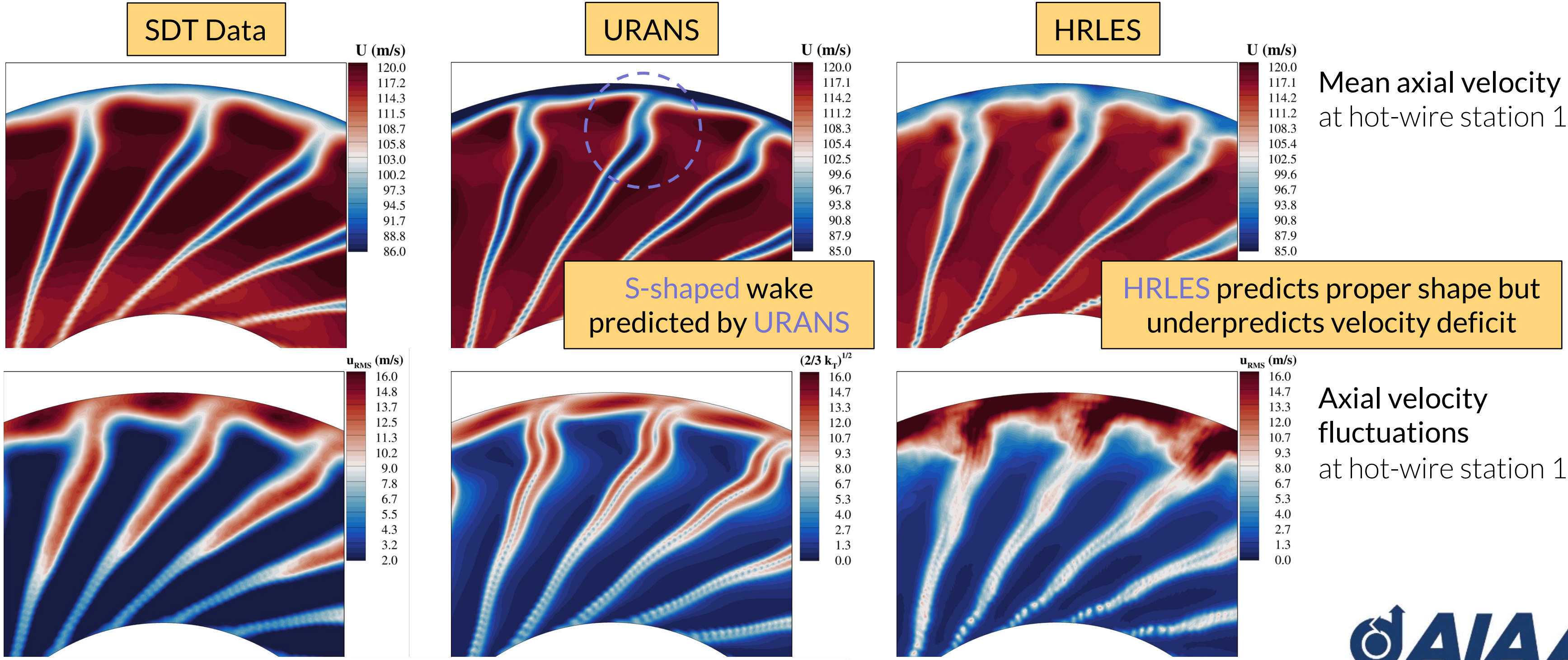

Mean axial velocity
at hot-wire station 1

Axial velocity fluctuations
at hot-wire station 1

Low-Speed (Approach) Condition

- Spectral content of the velocity field in the interstage region
  - Tonal content in agreement with SDT data for both URANS and HRLES
  - Broadband content near the casing captured up to BPF_2 in HRLES

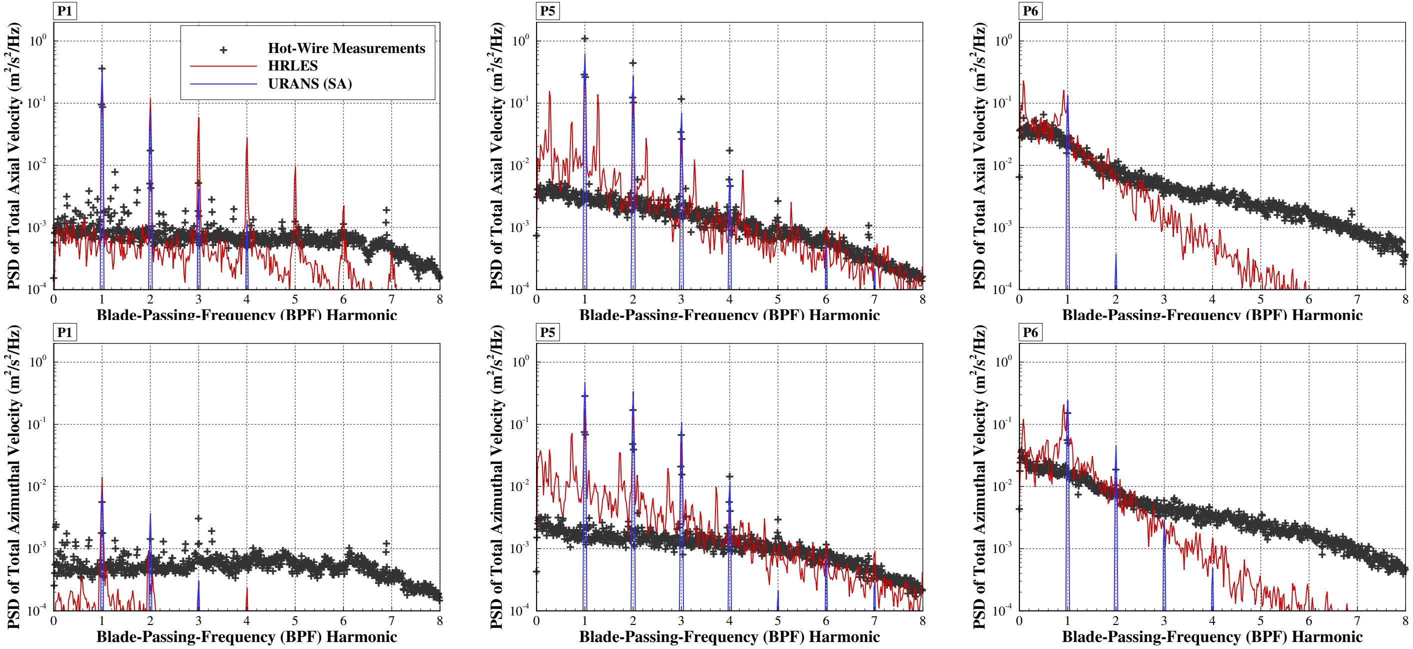

Spectral data extraction locations

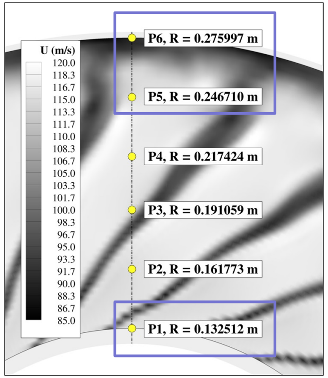

SHAPING THE FUTURE OF AEROSPACE

High-Speed (Take-Off) Condition

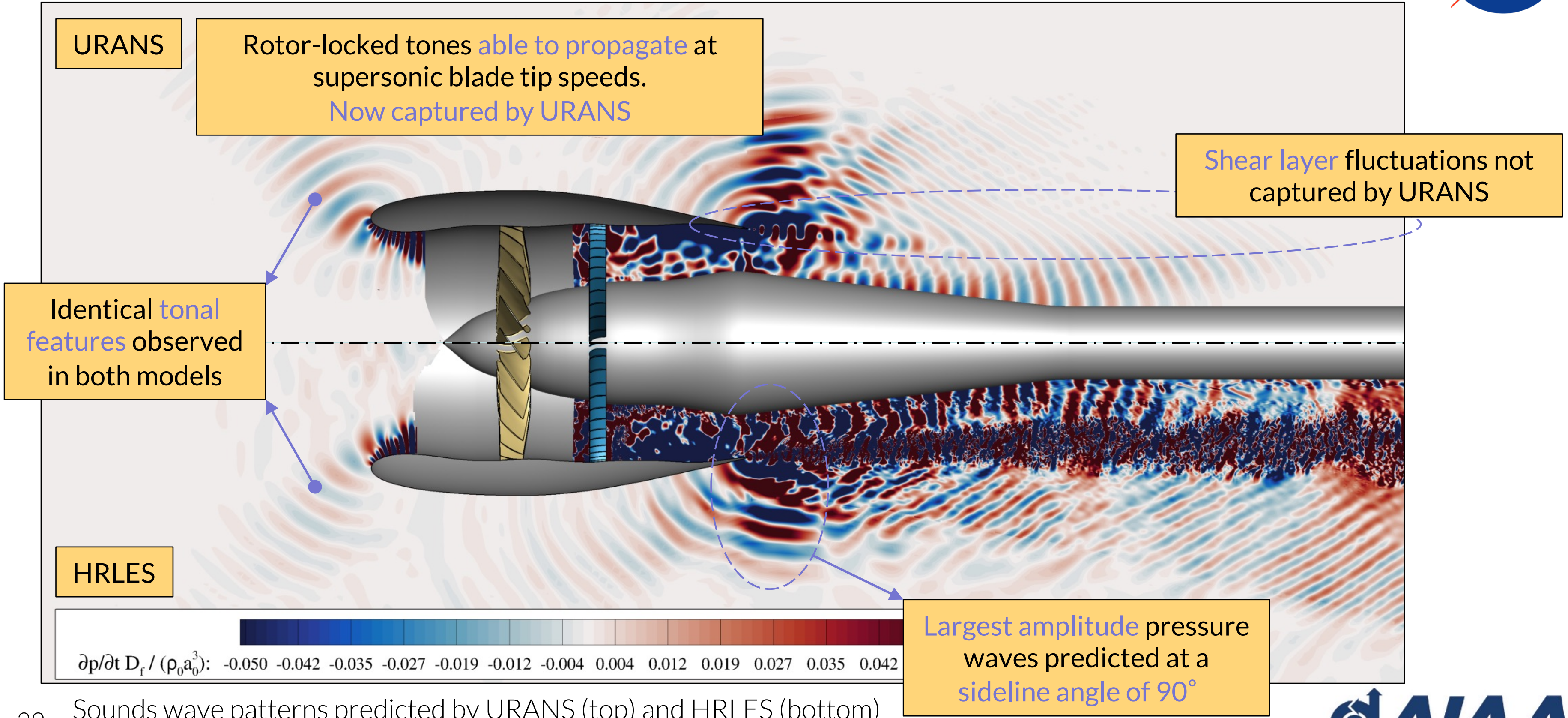

Sounds wave patterns predicted by URANS (top) and HRLES (bottom)

High-Speed (Take-Off) Condition

Tim Sandstrom render video at high-speed

Video legend

High-Speed (Take-Off) Condition

- Similar to the low-speed regime, performance metrics show excellent agreement with SDT data (< 2%):

Case	Mass Flow Rate		Total Pressure Ratio		Total Temperature Ratio	
	Value [kg/s]	Δ †	Value	Δ	Value	Δ
SDT Data	**43.998**	-	**1.490**	-	**1.137**	-
URANS (SA)	44.787	+1.79 %	1.497	+0.47 %	1.136	+0.09 %
HRLES-L	44.523	+1.19 %	1.492	+0.13 %	1.135	-0.18 %
HRLES -NL	44.560	+1.28 %	1.493	+0.20 %	1.135	-0.18 %

†Percent difference relative to the SDT data

Summary and Future Work

- URANS captures the mean flow in the interstage almost as well as, and sometimes better than, hybrid RANS/LES
- Both methods struggle to predict the flow-field downstream of the blade tip
- URANS fails to capture the broadband noise, which is dominant in the low-speed regime
- The results support the use of the newly-implemented sliding mesh technique to simulate turbomachinery components in relative rotating motion using the LAVA solver framework
- The acoustic signature of the fan stage produced by both flow models will be presented in Part II of this research.

Acknowledgements

- This work was funded by NASA Aeronautics Research Mission Directorate's (ARMD) Advanced Air Transport Technology (AATT) project under Advanced Air Vehicles Program (AAVP) and the Transformational Tools and Technologies (T^3) project under the Transformative Aeronautics Concepts Program (TACP).
- Computer time was provided by the NASA Advanced Supercomputing (NAS) facility at NASA Ames Research Center (ARC)
- The authors would like to thank and acknowledge Dr. Edmane Envia from NASA Glenn Research Center (GRC) for providing the SDT experimental dataset and valuable insight into interpretation of the data, Christopher Hughes from NASA GRC for the colored images of the SDT experiment, Dr. Timothy Chau and James Koch from NASA ARC for the internal review

AMERICAN INSTITUTE OF
AERONAUTICS AND ASTRONAUTICS